Robust Active Magnetic Bearing Control Using Stabilizing Dynamical Compensators

G.R. Duan, Z.Y. Wu, C.M. Bingham and D. Howe
Electrical Machines and Drives Group, Department of Electrical and Electronic Engineering,
The University of Sheffield, Mappin Street, Sheffield S1 3JD, UK.

Abstract: The robust control of active magnetic bearings, based on a linearised interval model, is considered. Through robust stability analysis, all the first-order robust stabilizing dynamical compensators for the interval system are obtained. Disturbance attenuation and minimum control effort are also addressed. The approach is applied to a high-speed flywheel supported by two active and two passive magnetic bearings. Simulation and experimental results both show that it is simple, effective, and robust.

Keywords: Magnetic bearings, interval systems, dynamical compensators, robust stabilization, disturbance attenuation, minimal control.

I. INTRODUCTION

Active magnetic bearings (AMBs) have several advantages over conventional bearings, and are being employed increasingly in a variety of applications [1]. However, two difficulties concerning magnetic bearing control involve system uncertainties and the difficulty of obtaining a good velocity signal [2]. In this paper, a basic AMB comprising two opposing electromagnets and a rigid rotor, as shown in Fig. 1, is considered. To cope with system parameter uncertainties, an interval model is employed. To avoid the use of a velocity feedback signal, a dynamical compensator, which uses only positional information, is utilised for control. By deriving a stability condition for the closed-loop system, a parameterisation of all the robust stabilising dynamical compensators for the interval system is obtained. By appropriately selecting the free parameters in the robust stabilizing controller, the H_2 norm of the transfer function from disturbance to output is made arbitrarily small over the system parameter intervals, and the H_∞ norm of the controller transfer function is made arbitrarily close to a lower bound. The proposed approach is applied to a high-speed flywheel supported by two active radial magnetic bearings and two passive axial magnetic bearings.

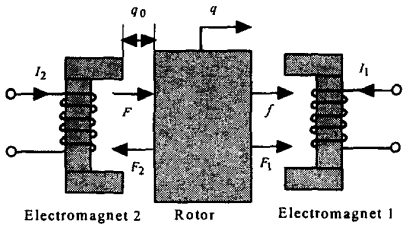

Fig. 1. Basic magnetic bearing

II. PLANT MODEL AND CONTROLLER

The dynamical mathematical model for the active magnetic bearing shown in Fig.1 can be established as:

$$m\ddot{q} = \frac{\mu_0 AN^2}{4}\left[\left(\frac{I_1}{q_0 - q}\right)^2 - \left(\frac{I_2}{q_0 + q}\right)^2\right] + f + F \qquad (1)$$

where m and q are, respectively, the mass (kg) and the position displacement (m) of the rotor; q_0 is the nominal air gap (m); $\mu_0 = 4\pi \times 10^{-7}$ H/m; A is the total pole-face area of each electromagnet (m^2); N is the number of turns per coil; I_1, I_2 are the currents in the coils (A); f is an unknown disturbance (N); and F is some known force acting on the rotor (N). When linearised at the equilibrium point $I_1 = I_2 = I_0$, $q = 0$, with the control diagram shown in Fig. 2, the above model (1) becomes

$$\ddot{q} - \omega^2 q = \sigma u + \frac{1}{m}(f + F) \qquad (2a)$$

where ω and σ are determined by I_0, q_0, and the system physical parameters, and u is the derived control action. Due to inaccuracies in the measurement of some of the physical parameters and changing environmental conditions, the parameters ω and σ are generally uncertain. Without loss of generality, however, it can be assumed that their values lie within some known intervals, viz.

$$\omega \in [\omega_1 \quad \omega_2], \quad \sigma \in [\sigma_1 \quad \sigma_2] \qquad (2b)$$

where ω_1, ω_2, σ_1 and σ_2 are known scalars satisfying

$$\omega_2 \geq \omega_1 > 0, \qquad \sigma_1 \leq \sigma_2 < 0 \qquad (2c)$$

If y is the measured value of q, then a general first-order output dynamical compensator for system (2) can be written in the form [3]:

$$\begin{cases} \dot{z} = k_{22} z + k_{21} y \\ u = k_{11} y + k_{12} z + k_f F \end{cases} \qquad (3a)$$

where $k_{ij}, i,j = 1,2$, are four scalar controller coefficients, to be designed, and the coefficient k_f is given by

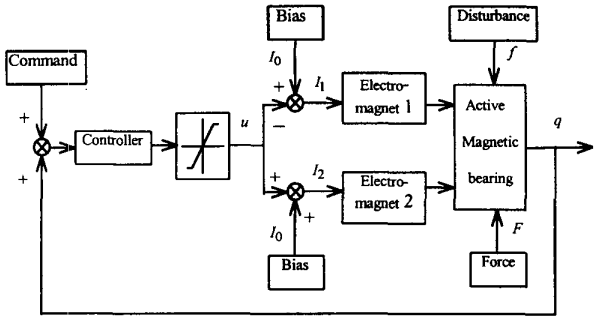

Fig. 2. Control System

$$k_f = -\frac{1}{m\sigma} = \frac{q_0^2}{\mu_0 A N^2 I_0} \tag{3b}$$

The resulting closed-loop system can subsequently be written in the state-space form:

$$\begin{cases} \dot{\xi} = A_{mc}\xi + d_{mc} f \\ y = c_m \xi \end{cases} \tag{4a}$$

with

$$A_{mc} = \begin{bmatrix} A_m + b_m k_{11} c_m & b_m k_{12} \\ k_{21} c_m & k_{22} \end{bmatrix} = \begin{bmatrix} 0 & 1 & 0 \\ \sigma k_{11} + \omega^2 & 0 & \sigma k_{12} \\ k_{21} & 0 & k_{22} \end{bmatrix} \tag{4b}$$

$$c_{mc} = [1 \quad 0 \quad 0], \quad d_{mc}^T = \begin{bmatrix} 0 & \frac{1}{m} & 0 \end{bmatrix} \tag{4c}$$

III. ROBUST STABILIZATION

The dynamical compensator (3) is said to be a *robust stabilizing compensator for the interval system* (2), or is said *to robustly stabilize the interval system* (2), if the matrix A_{mc} given in (4b) is Hurwitz stable for all ω and σ satisfying (2b) and (2c). For robust stabilization of system (2) with the dynamical compensator (3), the following result holds.

Theorem 1: All the robust stabilizing compensators in the form of (3), for system (2), are given by

$$\begin{cases} k_{11} = -\frac{1}{\sigma_2}\left(\omega_2^2 + \alpha\right) \\ k_{22} = -\beta \\ k_{12} = \gamma \\ k_{21} = \frac{\alpha\beta\tau}{\sigma_2 \gamma} \end{cases} \tag{5a}$$

with α, β, γ and τ being real scalars satisfying

$$\alpha > 0, \ \beta > 0, \ \gamma \neq 0, \ 0 < \tau < 1 \tag{5b}$$

IV. DISTURBANCE ATTENUATION

The disturbance attenuation specification can be expressed as follows:

$$N' = \sup_{\substack{\omega \in [\omega_1 \ \omega_2] \\ \sigma \in [\sigma_1 \ \sigma_2]}} \left\| c_{mc}\left(sI - A_{mc}\right)^{-1} d_{mc} \right\|_2^2 \leq \varepsilon_0 \tag{6}$$

where ε_0 is an arbitrary positive number.

Theorem 2: Let ε_0 be an arbitrary positive scalar, then, the robust stabilizing dynamical compensator for the interval system (2), given by (3) and (5),

(i) guarantees the specification in (6) if the parameter α is taken as

$$\alpha = \frac{1 + \sqrt{1 + 8\varepsilon_0 \beta^3 \frac{\tau}{1-\tau}}}{4\varepsilon_0 \beta \tau} + \theta^2 \tag{7}$$

(ii) guarantees the specification in (6), and minimises the index N' with respect to β, if the parameters α and β are taken as

$$\begin{cases} \alpha = \frac{1}{\sqrt[3]{\varepsilon_0^2 \tau^2 (1-\tau)}} + \theta^2 \\ \beta = \sqrt{\left(\frac{1-\tau}{\varepsilon_0 \tau}\right)^{\frac{2}{3}} + \theta^2 (1-\tau)} \end{cases} \tag{8}$$

(iii) guarantees the specification in (6), and minimises the index N' with respect to both β and τ, if the parameters α, β and τ are taken as

$$\begin{cases} \alpha = 3\left(\frac{1}{\sqrt[3]{2\varepsilon_0}} + \theta^2\right)^2 \\ \beta = \frac{1}{\sqrt[3]{2\varepsilon_0}} + \theta^2 \\ \tau = \frac{2}{3} \end{cases} \tag{9}$$

where in (7)-(9), θ is an arbitrary real scalar.

V. MINIMUM CONTROL EFFORT

The controller given in (3) can be written, in the frequency domain, as follows:

$$u(s) = G_{uy}(s) y(s), \qquad G_{uy}(s) = \left(\frac{k_{12}k_{21}}{s - k_{22}} + k_{11}\right) \tag{10}$$

In order to facilitate a small control effort, the following index is proposed:

$$J = \left\| \frac{k_{12}k_{21}}{s - k_{22}} + k_{11} \right\|_\infty \tag{11}$$

which can be shown to have the greatest lower bound

$$J_{glb} = \frac{\omega_2^2}{|\sigma_2|} \tag{12}$$

The control effort specification can, therefore, be expressed as

$$J - \frac{\omega_2^2}{|\sigma_2|} = \left\| \frac{k_{12}k_{21}}{s - k_{22}} + k_{11} \right\|_\infty - \frac{\omega_2^2}{|\sigma_2|} \le \varepsilon_u \tag{13}$$

where ε_u is an arbitrarily given positive scalar.

Theorem 3: Let ε_0 and ε_u be two arbitrary positive scalars. Then, the robust dynamical stabilizing compensator given by (3) and (5) for the interval system (2), guarantees the specification in (6), and at the same time,

(i) meets the control effort restriction (13) if α is taken as in (7) and τ is chosen as

$$\tau = \frac{\beta^2 + |\sigma_2|\varepsilon_u}{\beta^2 + |\sigma_2|\varepsilon_u\left(1 + 2|\sigma_2|\beta\varepsilon_0\varepsilon_u\right)} \tag{14}$$

(ii) meets the control effort restriction (13), and minimises the index N' with respect to β if

$$\begin{cases} \alpha = \dfrac{1 + \varepsilon_0\sqrt{(\varepsilon_u|\sigma_2|)^3}}{\varepsilon_0\sqrt{\varepsilon_u|\sigma_2|}}, \quad \beta = \sqrt{\varepsilon_u|\sigma_2|} \\ \tau = \dfrac{1}{1 + \varepsilon_0\sqrt{(\varepsilon_u|\sigma_2|)^3}} \end{cases} \tag{15}$$

VI. SIMULATION AND EXPERIMENTS

The proposed approach has been applied to a flywheel energy storage system which is being developed for use in urban electric vehicles. A schematic of the flywheel is shown in Fig.3. The flywheel rim is supported by two active radial magnetic bearings, whose normal air gap is q_0=0.4 mm, and two passive axial bearings. The active bearings have a homopolar topology, each electromagnet comprising two abutting E-shaped cores. On the vertical axis, the pole-face area of each core is 10.4 x 10^{-4}m^2, whilst on the horizontal axis the pole-face area is 5.2 x 10^{-4}m^2. Each core carries a coil having 40 turns. The mass of the flywheel rim is 12 kg. The upper bounds for the two parameters ω and σ in the linear model (2) for the two electromagnets on the vertical axis were chosen to be ω_2=390 and $\sigma_2 = -4.5$, while those for the electromagnets on the horizontal axis were chosen to be ω_2=280 and $\sigma_2 = -2$. Based on these values and Theorem 3, robust controllers in the form of (3) for the electromagnets on both the vertical and horizontal axes were obtained. The resulting coefficients are shown in Table 1.

Applying controller (3), with the coefficients given in Table 1, to the non-linear system (1) yields the non-linear closed-loop control system. Assuming m =6kg for both the vertical and horizontal axes, simulations of the non-linear closed-loop systems for both axes were carried out, and satisfactory results obtained. The controllers were then implemented digitally on a TMS320C40 DSP-based

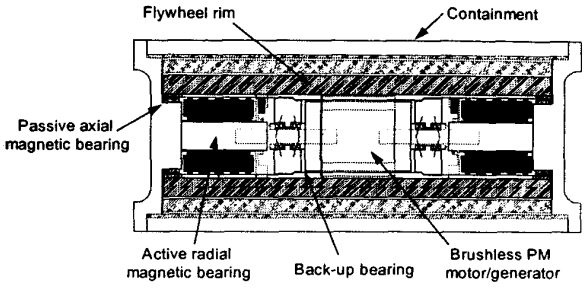

Fig. 3 Schematic of flywheel unit

hardware platform. Various experiments have been carried out to validate their performance. By way of example, Fig.4 shows the initial responses when all four electromagnets on each magnetic bearing are energised simultaneously, x1 and x2 being the horizontal position of the flywheel rim, and y1 and y2 being the vertical position. The results clearly demonstrate the stability attributes of the controller for this system. Interestingly, y1 also indicates the presence of a non-minimum phase zero. This is a multi-variable phenomena, and is due to imperfect matching of the speed of response of the bearings at each end of the flywheel rim.

TABLE 1. CONTROLLER COEFFICIENTS

Coefficients	Vertical	Horizontal
k_{11}	256022	539200
k_{12}	10000	10000
k_{21}	-111111	-250000
k_{22}	-5000	-5000
k_f	1.610880E-2	1.610880E-2

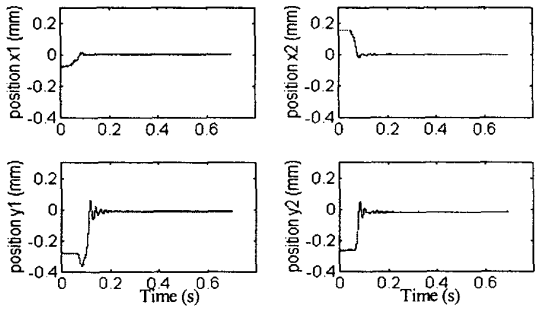

Fig. 4 Initial energisation of flywheel bearing system

VII. REFERENCES

[1] M. Dussaux, "The industrial applications of active magnetic bearing technology," *Proceedings of the Second International Symposium on Magnetic Bearings,* July 12-14, 1990, pp.33-38.

[2] J. Levine, J. Lotton, and J.C. Ponsart, "A nonlinear approach to the control of magnetic bearings," *IEEE Transactions on Control Systems Technology*, vol. 4, no. 5, 1996, pp.524-544

[3] G. R. Duan, "Robust eigenstructure assignment via dynamical compensators," *Automatica*, vol. 29, no. 2,, 1993, pp.469-474.